Boletim da Sociedade Astronômica Brasileira, **34**, no. 1, 38-43

Investigating the rotational evolution of solar-type stars with the Toulouse-Geneva Evolution Code

Bernardo F. O. Gonçalves[1], Rafael R. Ferreira[1], Matthieu Castro[1] & José Dias do Nascimento Jr.[1]

[1] Universidade Federal do Rio Grande do Norte (UFRN);
e-mail: odlavson@fisica.ufrn.br; e-mail: odlavson.pesquisa@gmail.com

Abstract. The rotation evolution of Sun-like stars is currently one of the most debated issues in the field of stellar physics. The discussion revolves around a possible decrease in the magnetic braking beginning about the age of the Sun, which would compromise the validity of the Skumanich law and the gyrochronology technique. In this scenario, it is important to carefully investigate if a decrease in the magnetic braking efficiency is a general phenomenon, otherwise assuming the risk of generalizing the existence of stellar internal processes that are not ubiquitous among solar-type stars. In this work, we study different samples of solar-type stars with the aid of the evolution models of the Toulouse-Geneva Evolution Code (TGEC). We study samples with seismological and isochronal ages and we added a final sample of low-activity stars with ages determined by chemical clocks, which gives us the possibility of discussing the relationship between weakened magnetic breaking and changes in the dynamo. We found that the sample with seismological data is not well constrained for a study about the rotation and magnetic evolution of the Sun. The sample of low-activity stars does seem to be affected by a decrease in magnetic braking despite differences in metallicity, although targets with higher metallicity seem to follow our evolution tracks better. At last, we found a mismatch between our rotation evolution tracks and the position of young stars. However, we have yet to test braking prescriptions that account for changes in magnetic morphology during stellar evolution.

Resumo. A evolução da rotação de estrelas semelhantes ao Sol é uma das questões atuais mais debatidas no campo da física estelar. A discussão gira em torno de uma possível diminuição da frenagem magnética a partir da idade do Sol, o que comprometeria a validade da lei de Skumanich e a técnica da girocronologia. Nesse cenário, é importante investigar com cuidado se uma diminuição na eficiência do freio magnético é um fenômeno universal, caso contrário assumindo o risco de generalizar a existência de processos estelares internos que não são onipresentes em estrelas do tipo solar. Neste trabalho, estudamos diferentes amostras de estrelas do tipo solar com o auxílio dos modelos de evolução do Toulouse-Geneva Evolution Code (TGEC). Estudamos amostras com idades sismológicas e de isócronas e adicionamos uma amostra final de estrelas de baixa atividade com idades determinadas por relógios químicos, o que nos dá a possibilidade de discutir a relação entre uma dimunição na frenagem magnética e mudanças no dínamo. Descobrimos que a amostra com dados sismológicos não está bem restrita para um estudo sobre a rotação e evolução magnética do Sol. A amostra de estrelas de baixa atividade parece ser afetada por uma diminuição no freio magnético apesar das diferenças na metalicidade, embora alvos com maior metalicidade pareçam seguir melhor nossos traçados evolutivos. Por fim, encontramos uma incompatibilidade entre nossos traçados de evolução da rotação e a posição das estrelas jovens. Contudo, ainda temos que testar as prescrições de freio que contabilizam as mudanças na morfologia magnética durante a evolução estelar.

Keywords. Stars: interiors – Stars: rotation – Stars: magnetic field – Stars: solar-type – Sun: rotation

1. Introduction

We are seeing a revolution happens in the field of observational astronomy. The technological advances of our time, together with the current computational capability for data analysis, are allowing the investigation of stellar parameters in thousands of stars. Among the technological instruments that are forging this revolution in the observational realm, we can cite the space telescopes built for the CoRoT mission (ESA) (Baglin et al. 2006), and for the subsequent Kepler/K2 mission (NASA) (Borucki 2010; Howell 2014), not to mention the space telescope built for the ongoing TESS mission (NASA) (Ricker et al. 2015), which represents the following generation of space telescopes. On top of that, the Gaia mission provides high precision photometry and parallaxes for billions of stars, helping the astrophysical community to better characterize stellar formation and the evolution of the galaxy, besides the physics and the evolution of stars and exoplanets (Gaia Collaboration et al. 2016, 2018).

In that scenario, the recent findings from the analysis of the high precision, high cadence, light curves observed by the NASA's satellites revealed some unexpected features of the evolution of stars, especially related to their rotation evolution. Some of the conclusions extracted from the photometric data analysis have put under serious stress our present theoretical understandings of how stars behave and evolve, and the problem of how rotation and magnetism are intertwined in the stellar interiors is becoming more and more complicated as new data come out (Metcalfe & van Saders 2017). Strangely enough — but predictable in some sense —, the revolution in observational astronomy may be leading to a crisis in the field of theoretical stellar physics. As presented in recent years by different authors (Finley & Matt 2017, 2018; Garraffo et al. 2018), a new understanding start to emerge toward the idea that the rotation evolution of solar-type stars could assume a different behavior due to changes in magnetic morphology, which have recently began to be verified by the usage of techniques such as Zeeman-Doppler Imaging (Metcalfe et al. 2019).

The problem we are currently addressing began with a mismatch between the data of young clusters and of old field Kepler stars plotted together in a rotation-age diagram. Angus et al. (2015) did not succeed in deriving a single gyrochronological relationship when including the Kepler data for old field stars, with seismic ages, together with the already known data from young open clusters (Gallet & Bouvier 2013; Gallet & Bouvier 2015). Before Angus et al. (2015), García et al. (2014) had al-

ready shown the Sun with a slightly higher rotation period than a sample of selected Kepler targets.

In the following year, van Saders et al. (2016) and Metcalfe et al. (2016) went a step further and proposed a radical shift in the stellar rotation evolution after the age of the Sun, which, in principle, would explain the anomalous old field Kepler stars, but would seriously compromise the validity of the Skumanich law (Skumanich 1972) and the age estimating technique known as gyrochronology (Barnes 2007). They proposed a weakening in the magnetic braking after $Ro \approx 2$, where Ro is the Rossby number ($Ro = P_{rot}/\tau_c$, where τ_c is the convective overturn time, see Noyes et al. 1984), which would be around the age of the Sun for a star with mass and metallicity close to the solar values. With models reproducing the shutdown of magnetic braking, van Saders et al. (2016) were capable of fitting the rotation evolution of a Kepler sample together with a group of old solar analogues. Since this is still an unresolved issue, it is important to continue to examine different methods of estimating stellar ages and to continue to test different stellar samples, so that we can have a clear picture of where we are standing in relation to the theory of rotation evolution of solar-type stars established, initially, by Weber & Davis (1967) and Skumanich (1972).

In this proceedings, we report our investigation of the rotation evolution of different samples of solar analogues and twins using rotating models computed with the Toulouse-Geneva Evolution Code (TGEC) (Hui-Bon-Hoa 2008; do Nascimento et al. 2009). We study three samples of solar analogues and twins together with a control sample of solar analogues with ages derived by gyrochronology.

2. Sample Selection

Intending to study how different samples of solar-type stars would behave in comparison to our solar rotation evolution tracks, we first selected three samples from the literature that use three different methods of computing the age estimates of stars. The first one is the sample of do Nascimento et al. (2020), which uses gyrochronology as the age estimation method of a solar analogues sample. This is a cross-matched sample between Kepler and Gaia data, which means the rotation of those stars comes from the photometric analysis of Kepler light curves.

The second sample comes from the work of Beck et al. (2017), which uses ages derived from seismological data and rotation periods also derived from the analysis of Kepler light curves. The third sample we studied is presented in the work of Yana Galarza et al. (2021). The ages are derived from isochrones and, then, submitted to Bayesian inference. Half the targets of this sample were observed by either TESS or Kepler (besides the observation from the Gaia satellite), which means that the rotation periods were also estimated using photometric analysis of light curves.

Finally, we added an additional group of stars to our analysis. This last sample is composed of low activity stars (Maunder minimum candidates) studied in the work of Lubin et al. (2010). The ages for some of these targets were estimated from isochrones in the work of Brewer et al. (2016), and photometric rotation periods, although available for some, are scarce for this sample. Therefore, we estimated the rotation periods for these stars using the equation of activity calibration defined by Noyes et al. (1984). Furthermore, we searched in the literature for another source of age estimation, besides isochrones, for the stars in the sample of Lubin et al. (2010). We have found several estimates coming from chemical clocks (Nissen et al. 2017; Spina et al. 2018; Chen et al. 2020; Casali et al. 2020), which are the ages used in this work.

3. Numerical Tools

3.1. Evolution Models

The models in this work use nuclear reaction rates from the analytical formula of the NACRE compilation (Angulo et al. 1999), while atomic screening factors are described by Bahcall et al. (1992). We use the opacity tables from the OPAL OPACITY CODE (Iglesias & Rogers 1996), complemented at low temperature by the molecular opacities of Alexander & Ferguson (1994). For the equation of state (EOS), we use the OPAL 2001 EOS tables (Rogers & Nayfonov 2002). The mixing length theory (MLT) (Böhm-Vitense 1958) is the treatment of convection chosen to compute our models. Finally, we use the Eddington relation as the prescription for the integration of the stellar boundary with its atmosphere, with the correction of the Hopf function (Hopf 1930) and following the coefficients given by the calibration of Krishna Swamy (1966).

The most relevant part to this work is related to the routines that treat the transport of angular momentum. While some evolution codes treat the transport of angular momentum in the radiative zone as a diffusive process (e.g., Paxton et al. 2013), the TGEC uses an advection-diffusion equation (Zahn 1992). In the theory of angular momentum transport laid out by Zahn (1992), it is assumed, due to empirical evidence, that there is an anisotropy in turbulent motions, with the horizontal motion being much more vigorous than the vertical one. For the vertical transport of angular momentum (ν_v), we use the prescription laid out in the work of Talon & Zahn (1997) and, for the horizontal transport of angular momentum (ν_h), we use the prescription described in Mathis et al. (2004).

Despite some tests we made with the wind prescription of Matt et al. (2015), the models used in this work were computed with the classical wind prescription of Kawaler (1988), which was later modified to account for the saturation of angular momentum loss with rotation rate (Chaboyer et al. 1995). We found an appreciable difference in the rotation evolution track for these two prescriptions only in the very beginning of evolution (< 0.7 Gyr). Since both prescriptions follow the Skumanich law on the main sequence, a match between the tracks in this region was expected.

In order to have at the solar age ($t_\odot = 4.57 \times 10^9$ yr) an angular velocity of $\Omega_\odot = 2.86 \times 10^{-6}$ rad/s at the solar equator, we calibrated the magnetic braking constant to the value of $K_\mathrm{w} = 2.06 \times 10^{30}$ erg. We considered the angular velocity of magnetic saturation at $\Omega_\mathrm{sat} = 11\Omega_\odot$, as defined in Amard & Matt (2020). The magnetic saturation was not reached during the calibration of the solar model. Moreover, we calibrate this model to obtain at the solar age ($t_\odot$), solar luminosity ($L_\odot = 3.846 \times 10^{33}$ erg/s), solar radius ($R_\odot = 6.9599 \times 10^{10}$ cm) and solar metallicity ([Fe/H] = 0.00 dex).

The models computed in this work also simulate the disk-locking phase at the very beginning of the stellar evolution (Gallet & Bouvier 2013; Gallet & Bouvier 2015; Amard et al. 2016). All the evolution tracks start with a rotation period of 7 days kept constant during the first 5 Myrs of stellar evolution. After that age, due to the dispersion of the protostellar cloud, the magnetic braking (due to stellar wind) starts to take effect as the star is now free to spin-up as it contracts towards the Zero Age Main Sequence (ZAMS). Then, the rotation period begins to increase slowly as the star continue losing angular momentum throughout its evolution.

We computed several evolution tracks changing only the initial mass and the initial metallicity of the model, this way building a grid of evolution tracks. Our grid extends in metallicity

from −0.40 to +0.40 dex and in mass from 0.80 $M_\odot$ to 1.20 $M_\odot$, in both cases iterating in steps of 0.04. To this grid, we applied our interpolation code to estimate stellar rotation period and stellar age of our sample stars, with 1σ uncertainty. This code uses a Markov chain sampler and takes as input observed T_{eff}, $L/L_\odot$ and [Fe/H] for each target. Besides rotation period and age, our interpolation code also estimates stellar mass and radius (Valle et al. 2014).

3.2. Spectroscopic Analysis

In order to better constrain the atmospheric parameters of Lubin et al. (2010) sample, we collected archive high-resolution spectra from different databases, including the databases of the instruments NARVAL, ESPaDOnS, ELODIE, SOPHIE and HARPS. The additional treatment of the spectra and especially the determination of the atmospheric parameters were done using the spectral analysis tool iSpec (Blanco-Cuaresma et al. 2014; Blanco-Cuaresma 2019). We used spectral synthesis as the method to compute the atmospheric parameters of these targets. For the targets of other samples, we did not compute atmospheric parameters but rather used their own estimates, which also come from spectroscopic analysis.

We always followed the same procedure for parameter determination. After verifying that the spectra were properly reduced — and applying our own scripts when the additional reduction was necessary —, we proceed to correct radial velocity e normalize the spectra. Next, we load the line mask with the specific spectral regions that are used during the spectral synthesis process and we select the spectral region that will be synthesized. The line mask we used is one of the standard line masks provided by iSpec, properly designed to be used with our choices of radiative transfer code and atomic line list. The region of spectral synthesis is the same for all cases, 480−680 *nm*, right at the center of the visible spectrum. Our choices for the radiative transfer code, atmospheric model, solar abundances and atomic line list are the following: SPECTRUM, MARCS GES (Gustafsson et al. 2008), Grevesse 2007 (Grevesse et al. 2007), VALD 300−1100 *nm*. The atmospheric parameters determined for the Lubin et al. (2010) objects are shown in Gonçalves et al. (2022).

For the sample of Lubin et al. (2010), we used in our analysis ages estimated by chemical clocks (Nissen et al. 2017; Spina et al. 2018; Chen et al. 2020; Casali et al. 2020), which is an uncorrelated means, with regards to our models, of estimating stellar ages. This relatively new method of estimating stellar ages rely on the precise measurement of the chemical abundance of certain elements and its correlation to the precise ages of some specific targets (in stellar clusters, for example), providing a way of calibrating a chemical clock for the estimation of ages in stars of the same spectral type and similar metallicity. This method requires a highly precise spectroscopic analysis of chemical abundances, which one of the most common chemical clocks currently used are the abundance ratios of [Y/Mg] and [Y/Al] (Casali et al. 2020).

4. Results

Since our evolution models follow the Skumanich law on the main sequence, as does, by design, the ages derived by gyrochronology, then we cannot make any further analysis for the sample of do Nascimento et al. (2020) in comparison to our rotation evolution models. However, it may serve as a control sample to our models and the mismatches between our evolution models and the targets of this sample, especially among young stars, should be granted a deeper investigation (Figure 1).

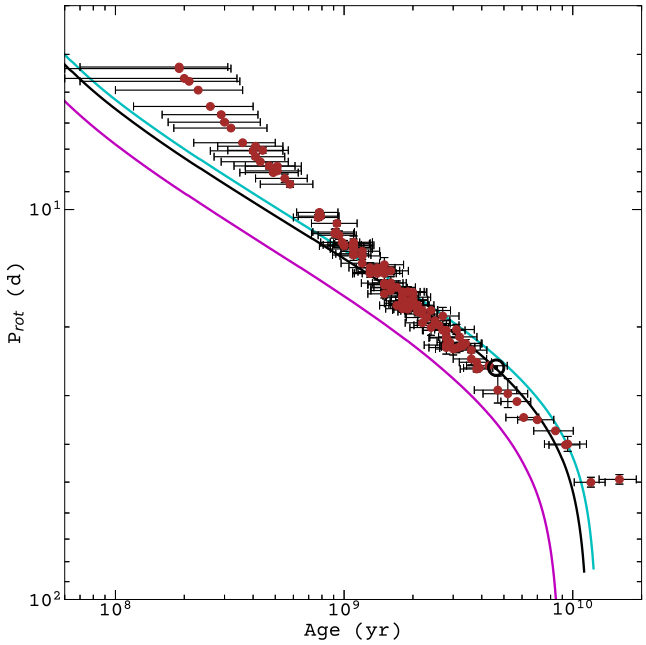

Figure 1. Period-age diagram for our control sample of do Nascimento et al. (2020). Solid lines are the evolution tracks of rotational models of $0.95M_\odot$ (cyan line) and $1.05M_\odot$ (magenta line), computed with [Fe/H] = 0.00 dex, besides the evolution track of our solar model (black line).

The other three samples are displayed together in the H-R diagram of Figure 2. It is possible to see clearly that the sample of Beck et al. (2017) (Figure 2, top) is the one that presents the greatest dispersion, indicating that these targets are quite different from the Sun. Most of them have high luminosities, perhaps indicating that some are main sequence F-type stars, beyond the Kraft break (Kraft 1967), or already evolved stars. Despite those targets being classified as solar analogues in the paper by Beck et al. (2017), we stress that we see a different picture revealed by Gaia photometry. We found that these targets present a rotation period that does not match our evolution tracks, presenting faster rotation periods than what we would expect for solar-type stars.

On the other hand, the targets selected by Yana Galarza et al. (2021) (Figure 2, middle) are the ones closest to the Sun in the H-R diagram, revealing their sample selection towards the search for solar twins and solar analogues. Those targets agree well with the evolution of the rotation periods of our tracks in the H-R diagram, except for a single outlier.

Lastly, the sample of low-activity stars of Lubin et al. (2010) (Figure 2, bottom) appears to be most solar-like, however with some outliers of large luminosity. It shows again the pattern identified in the targets of Beck et al. (2017), where the targets seem to be rotating faster than they should, according to our evolution models.

In Figure 3, we investigate the influence of stellar metallicity on rotation evolution for each sample. For the Beck et al. (2017) sample, it turns out these stars are very heterogeneous, as seen in the H-R diagram of Figure 2. This lack of homogeneity makes it difficult to derive a clear conclusion of Figure 3 (top). We regard this sample as not well constrained for this analysis. We also verified that an interpolation of our stellar evolution models

estimates higher rotation periods for this sample, while we cannot identify this same bias for the age estimates (Gonçalves et al. 2022).

For the young stars of Yana Galarza et al. (2021), Figure 3 (middle), it is also not possible to identify a clear picture regarding rotation period and metallicity. The interpolation over our grid of evolution tracks estimates higher rotation periods and higher ages for this sample (Gonçalves et al. 2022). As seen in the sample of do Nascimento et al. (2020), the youngest stars are located above our 0.95 $M_{\odot}$ track.

While for the two previous samples we used the ages and the rotation periods provided by Beck et al. (2017) and Yana Galarza et al. (2021), for the sample of Lubin et al. (2010) we used ages given by chemical clocks and rotation periods derived using the activity calibrations of Noyes et al. (1984) with our own activity estimations for those targets (R. R. Ferreira, in preparation). For the plot of Figure 3 (bottom), we applied a constraint in T_{eff} and logg to investigate the metallicity effect only for the stars that are most similar to the Sun. We constrained T_{eff} to the window of 5777 ± 200 K and logg to the window of 4.1 to 4.6. The stars represented with crosses in Figure 3 (bottom) are outside at least of one of those parameter ranges. The result this time show something more closely aligned to what is shown in the paper by Amard & Matt (2020), with the stars with higher metallicities staying closer to our rotation evolution tracks, while stars with lower metallicity deviating more strongly. Overall, the interpolation over our grid of stellar evolution models estimate higher rotation periods and higher ages for the stars of this sample (Gonçalves et al. 2022).

5. Conclusion

We analyzed the rotation evolution of three samples of solar-type stars coming from three different papers: Beck et al. (2017), Yana Galarza et al. (2021) and Lubin et al. (2010). Even though the sample of Beck et al. (2017) seems very heterogeneous and composed by some very high luminosity stars, making it difficult to conclude anything, we found that the low-activity stars of Lubin et al. (2010) present lower rotation periods than predicted by our model. The hypothesis behind this result is that a transition in the stellar dynamo may be underway for those targets, which would lead to changes in the stellar magnetic field morphology followed by a decrease in the efficiency of magnetic braking (Metcalfe et al. 2016, 2019). We found a point of contention between our evolution models and the young solar analogues of Yana Galarza et al. (2021), which needs to be further investigated. However, the paper by Garraffo et al. (2018) shed a light to the idea that changes in magnetic morphology in the earlier part of the rotation evolution can also be significant, which could solve this issue.

Based on our current knowledge, discrepancies observed between our evolution models and the samples analyzed could be solved if we implemented a form of magnetic braking that takes into account how changes in magnetic morphology affect the rate of angular momentum loss (Finley & Matt 2017, 2018; Garraffo et al. 2018). We intend to test those prescription of magnetic braking in our evolution code, since the current prescription was designed for a fixed magnetic field morphology. In the paper written regarding this work (Gonçalves et al. 2022), we tested an empirical reduction of the braking parameter by a factor of 10, showing that it is sufficient to account for most of the observations of our samples. However, the validity of such a range of magnetic braking values needs to be further investigated.

The rotation evolution of solar-type stars will continue to be studied so that we are able to understand in a deeper sense how this fundamental stellar property is intertwined with the magnetic phenomena. Until we get this relationship right, methods of estimating stellar ages such as gyrochronology are hindered, since we cannot safely determine which group of solar-type stars are not affected by a decrease in magnetic braking due to changes in the solar dynamo and magnetic field topology.

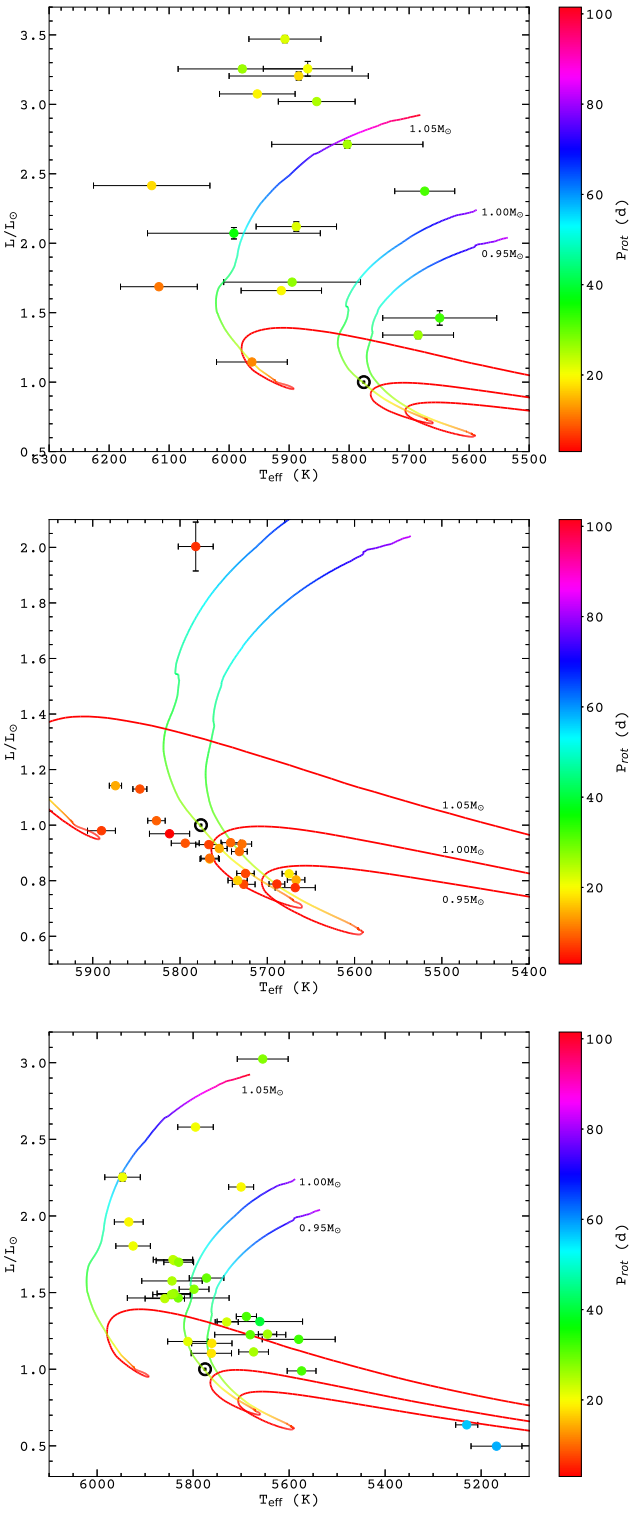

Figure 2. H-R diagram with a rotation pallet for both targets and evolution tracks. From top to bottom: Beck et al. (2017) sample, Yana Galarza et al. (2021) sample and Lubin et al. (2010) sample.

Acknowledgements. BFOG thanks the financial support of CAPES during the course of his doctorate.

References

Alexander, D. R., & Ferguson, J. W. 1994, ApJ, 437, 879
Amard L., Palacios A., Charbonnel C., Gallet F., Bouvier J., 2016, A&A, 587, A105
Amard, L., & Matt, S. P. 2020, ApJ, 889, 108
Angulo, C., Arnould, M., Rayet, M., et al. 1999, NuPhA, 656, 3
Angus, R., Aigrain, S., Foreman-Mackey, D., & McQuillan, A. 2015, MNRAS, 450, 1787
Baglin A., Auvergne M., Barge P., Deleuil M., Catala C., Michel E., Weiss W., COROT Team 2006, in Fridlund M., Baglin A., Lochard J., Conroy L., eds, ESA Special Publication Vol. 1306, The CoRoT Mission Pre- Launch Status - Stellar Seismology and Planet Finding. p. 33
Bahcall J. N., Pinsonneault M. H., 1992, Reviews of Modern Physics, 64, 885
Barnes, S. A. 2007, ApJ, 669, 1167
Beck, P. G., do Nascimento, J.-D., Duarte, T., et al. 2017, A&A, 602, A63
Blanco-Cuaresma, S., Soubiran, C., Heiter, U., et al. 2014, A&A, 569, A111
Blanco-Cuaresma, S. 2019, MNRAS, 486, 2075
Borucki W. J., et al., 2010, Science, 327, 977
Brewer, J. M., Fischer, D. A., Valenti, J. A., et al. 2016, ApJS, 225, 32
Böhm-Vitense, E. 1958, Zeit. Astrophys., 46, 108
Casali, G., Spina, L., Magrini, L., et al. 2020, A&A, 639, A127
Chaboyer, B., Demarque, P., & Pinsonneault, M. H. 1995, ApJ, 441, 865
Chen, X., Ge, Z., Chen, Y., et al. 2020, ApJ, 889, 157
do Nascimento Jr., J. D., Castro, M., Meléndez, J., et al. 2009, A&A, 501, 687
do Nascimento, J.-D., Jr., de Almeida, L., Velloso, E. N., et al. 2020, ApJ, 898, 173
Finley, A. J. & Matt, S. P. 2017, ApJ, 845, 46
Finley, A. J. & Matt, S. P. 2018, ApJ, 854, 78
Gallet, F. & Bouvier, J. 2013, A&A, 556, A36
Gallet, F., & Bouvier, J. 2015, A&A, 577, A98
Gaia Collaboration, Prusti, T., de Bruijne, J. H. J., et al. 2016, A&A, 595, A1
Gaia Collaboration, Brown, A. G. A., Vallenari, A., et al. 2018, A&A, 616, A1
García, R. A., Ceillier, T., Salabert, D., et al. 2014, A&A, 572, A34
Garraffo, C., Drake, J. J., Dotter, A., et al. 2018, ApJ, 862, 90
Gonçalves, B. F. O., Ferreira, R. R., Castro, M., et al. 2022, ApJ (submitted)
Grevesse, N., Asplund, M., & Sauval, A. J. 2007, Space Sci. Rev., 130, 105
Gustafsson, B., Edvardsson, B., Eriksson, K., et al. 2008, A&A, 486, 951
Hopf, E. 1930, MNRAS, 90, 287
Howell, S. B., Sobeck, C., Haas, M., et al. 2014, PASP, 126, 398
Hui-Bon-Hoa A., 2008, Ap&SS, 316, 55
Iglesias, C. A., & Rogers, F. J. 1996, ApJ, 464, 943
Kawaler, S. D. 1988, ApJ, 333, 236
Kraft, R. P. 1967, ApJ, 150, 551
Krishna Swamy, K. S. 1966, ApJ, 145, 174
Lubin, D., Tytler, D., & Kirkman, D. 2010, ApJ, 716, 766
Mathis, S., Palacios, A., & Zahn, J.-P. 2004, A&A, 425, 243
Matt, S. P., Brun, A. S., Baraffe, I., Bouvier, J., & Chabrier, G. 2015, ApJ, 799, L23
Metcalfe, T. S., Egeland, R., & van Saders, J. 2016, ApJ, 826, L2
Metcalfe, T. S. & van Saders, J. 2017, Sol. Phys., 292, 126
Metcalfe, T. S., Kochukhov, O., Ilyin, I. V., et al. 2019, ApJ, 887, L38
Morel, P., van't Veer, C., Provost, J., et al. 1994, A&A, 286, 91
Nissen, P. E., Silva Aguirre, V., Christensen-Dalsgaard, J., et al. 2017, A&A, 608, A112
Noyes R. W., Hartmann L. W., Baliunas S. L., Duncan D. K., Vaughan A. H., 1984, ApJ, 279, 763
Paxton, B., Cantiello, M., Arras, P., et al. 2013, ApJS, 208, 4
Ricker G. R., et al., 2015, Journal of Astronomical Telescopes, Instruments, and Systems, 1, 014003
Rogers, F. J., & Nayfonov, A. 2002, ApJ, 576, 1064
Skumanich, A. 1972, ApJ, 171, 565
Spina, L., Meléndez, J., Karakas, A. I., et al. 2018, MNRAS, 474, 2580
Talon, S., & Zahn, J.-P. 1997, A&A, 317, 749
Valle, G., Dell'Omodarme, M., Prada Moroni, P. G., et al. 2014, A&A, 561, A125
van Saders, J. L., Ceillier, T., Metcalfe, T. S., et al. 2016, Nature, 529, 181
Weber, E. J. & Davis, L. 1967, ApJ, 148, 217
Yana Galarza, J., López-Valdivia, R., Lorenzo-Oliveira, D., et al. 2021, MNRAS, 504, 1873
Zahn, J.-P. 1992, A&A, 265, 115

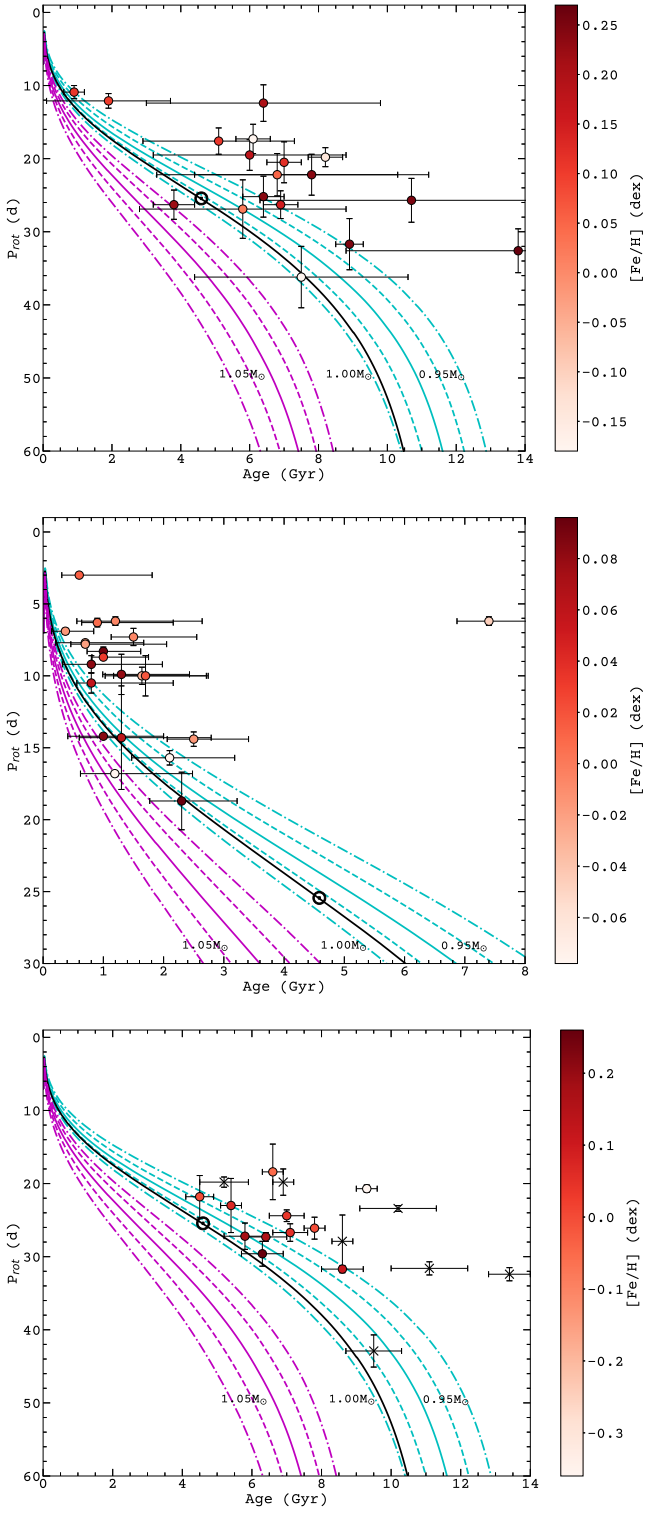

Figure 3. Period-age diagram with a metallicity pallet. The black solid line is our solar model, while other solid lines represent tracks computed with [Fe/H] = 0.00 dex. Dashed lines are tracks computed with [Fe/H] = ±0.05 dex and dash-dotted lines are tracks computed with [Fe/H] = ±0.10 dex. From top to bottom: Beck et al. (2017) sample, Yana Galarza et al. (2021) sample and Lubin et al. (2010) sample.